Korean J. Chem. Eng., 39(5), 1135-1145 (2022)
DOI: 10.1007/s11814-021-1032-9

pISSN: 0256-1115
eISSN: 1975-7220

Drying characteristics of thermally pre-treated Cobra 26 F1 tomato slabs and applicability of Gaussian process regression-based models for the prediction of experimental kinetic data

Oladayo Adeyi*,†, Emmanuel Olusola Oke*, Abiola John Adeyi,***, Bernard Iberzim Okolo*, Abayomi Olusegun Olalere****, John Adebayo Otolorin*, Ayomide Adeola*****, Brown Dagogo*****, Akinola David Ogunsola**, and Sunday Oladunni******

*Department of Chemical Engineering, Michael Okpara University of Agriculture, PMB 7267, Umudike, Abia State, Nigeria
**Department of Mechanical Engineering, Ladoke Akintola University of Technology PMB 4000, Ogbomoso, Oyo State Nigeria
***Forest Research Institute of Nigeria, PMB 5054, Jericho Ibadan, Oyo State, Nigeria
****Analytical Biochemistry Research Centre (ABrC), Universiti Sains Malaysia (USM), 11800, Gelugor, Penang, Malaysia
*****Department of Chemical Engineering, Landmark University, P.M.B 1001, Omu-Aran, Kwara State, Nigeria
******Department of Chemical Engineering, Ladoke Akintola University of Technology PMB 4000, Ogbomoso, Oyo State Nigeria

(*Received 16 April 2021 • Revised 4 November 2021 • Accepted 29 November 2021*)

Abstract−The drying characteristics of unblanched (UB), steam blanched (SB) and hot water blanched (WB) Cobra 26 F1 tomatoes were investigated at drying temperature of 40, 50, 60 and 70 °C and constant air velocity of 1.2 m/s in a convective oven. Gaussian process regression (GPR)-based models defined with squared-exponential kernel (GPR-SE), rational quadratic kernel (GPR-RQ), Matérn 5/2 kernel (GPR-M 5/2) and exponential kernel (GPR-Ex) were employed to model and predict experimental kinetic data of UB, SB and WB samples. Blanching and increased drying temperature reduced the drying time. The effective moisture diffusivity, activation energy, total and specific energy requirement for UB, SB and WB ranged between 3.6466 E -10 - 2.5526 E -09 m^2/s, 27.86-43.65 kJ/mol, 7.08-18.33 kW-h and 1,069.12-2,768.80 kW-h/kg, respectively. Increased drying temperature and pre-treatment reduced activation energy, total and specific energy requirements of Cobra 26 F1 tomatoes. Investigated GPR-based models were suitable for modelling and prediction of experimental kinetic data of Cobra 26 F1 tomatoes, GPR-M 5/2 was, however, marginally better. Hence, GPR-based models showed high suitability in handling multi-dimensional drying variables and can be used for developing robust controllers applicable in auto-monitoring and control of Cobra 26 F1 tomatoes industrial drying.

Keywords: Cobra 26 F1 Tomatoes, Gaussian Process Regression-based Models, Steam Blanched and Hot Water Blanched, Thermal Pre-treatment

INTRODUCTION

Tomatoes are the edible fruits produced by the plant *Solanum lycopersicum* and one of the most popular vegetables grown all over the world [1]. Tomatoes possess powerful antioxidants such as lycopene, lutein, and beta-carotene, and they are also good sources of folates and vitamin C [2]. High consumption of tomatoes has been linked to reduced risk of cancer, blood pressure and diabetes. Tomato intake also improves heart health, eye health, constipation and skin health. There are, however, over ten thousand (10,000) tomato cultivars with widely distinctive fruit characteristics in color, size, shape, maturity, resistance to disease, leaf type and growth. Among the hybrid varieties that is very popular and acceptable in Nigeria for high vigor and disease resistance, good productivity and early maturity is Cobra 26 F1. Cobra 26 F1 tomato is a medium sized square fruit with average weight of between 80 and 90 g. The fruits have uniform red or pink coloration, good firmness and relatively high conservation. However, high moisture content of tomato fruit increases its susceptibility to spoilage during storage and thus leads to increased post-harvest losses. One of the oldest and most widely studied methods of preserving and enhancing the shelf-life of agricultural produce in the literature is drying [3-6]. Drying of fruits and vegetables also increases the economic value of agricultural produce and is recently fast becoming a profitable commercial venture in Nigeria.

Drying is a process of moisture removal that achieves water activity value reduction and physicochemical and microbiological stability in the product [7]. Drying as a method removes humidity through simultaneous heat and mass transfer to achieve extended product shelf-life, reduced packaging cost, improved appearance, lighter weight transportation and smaller storage space [8,9]. The hot air drying method, which involves blowing heated air over food materials to remove moisture, of agricultural produce has been extensively studied [6,9-12] and identified as an efficient method

†To whom correspondence should be addressed.
E-mail: adeyioladayo350@yahoo.com

since heat and mass transfer can be controlled in an enclosed system during the progress of drying operation to achieve the desired qualities [13]. Other advantages of hot air drying include high ratio of heat and mass transfer, steady oven temperature, and high drying capacity [14]. Drying characteristics of agricultural produce are profoundly affected by air temperature, time, relative humidity, product size, air velocity, type of drying equipment and sample pre-treatment method [6,9,11].

Agricultural produce is pre-treated to speed up the drying process and preserve product quality [15]. Two of the widely investigated pre-treatment methods for fresh cut agricultural produce prior to drying operation are the chemical method, which involves dipping the material in chemical solutions, and blanching method, by thermal treatment either in water or steam. Chemical pre-treatment method has been reported to overcome the wax barrier present in fruits and vegetables [10] during drying and suppress browning [16]. Chemical solutions such as calcium chloride, sodium chloride, sodium chloride sucrose, and alkaline ethyl oleate solution have been used to pre-treat tomatoes [10,16]. However, government legislations and bans on some chemicals and consumer health awareness demanded for alternative pre-treatment methods [17]. Steam blanching and water blanching have, however, remained popular commercial pre-treatment methods because they are easy to establish and implement [17] and are cost effective and non-hazardous. Blanching as a form of thermal pre-treatments has been reported to prevent loss of color by inactivating enzymes and reduce drying time by relaxing tissue structure [6]. Blanching also yields good quality dried products [18].

Understanding of the drying process is of great importance for the purpose of precise monitoring and control of industrial dryers. Hence, process models give insight into the process and can be used for predicting future outcomes [19]. Drying data are inherently non-linear due to many operating variables affecting the drying process; hence, a robust methodology that can handle multi-dimensional variables typical of drying operation is necessary. Artificial intelligence (AI) modelling approaches have lately received considerably high attention and have played a key role in this regard. AI has been successfully used with high accuracy to model the non-linearity found in drying data and AI has found applications in the development of robust controller for auto-monitoring and control of industrial processes. Hence, intelligent machine learning techniques, such as artificial neural networks (ANN), adaptive neuro fuzzy inference system (ANFIS) and fuzzy logic (FL)) have recorded high success in modeling and predicting drying data and inherent properties of agricultural products [11,14,20,21]. Gaussian process regression (GPR) modeling is an intelligent non-parametric and flexible machine learning technique that is recently gaining popularity due to its high accuracy and conceptual simplicity [19]. The GPR model is a versatile, having many different kernels, model whose prediction is probabilistic in nature. Although the GPR approach is relatively new, it has been used for adaptive quality monitoring in batch processes [22], forecasting of dam deformation [23], modelling of pan evaporation [24] and in global horizontal irradiance forecasting [25].

Tomato drying in Nigeria is fast becoming a lucrative commercial investment, and the Cobra 26 F1 tomato stands a greater chance as a feedstock because of its recent acceptability and subsequent large cultivation in Nigeria. Hence, the need to determine drying characteristics of Cobra 26 F1 tomatoes for optimum economic processing and investigate appropriateness of GPR, AI approach useful in the design of a robust controller for monitoring and control of Cobra 26 F1 tomatoes industrial drying. Cobra 26 F1 tomatoes are a hybrid variety with inherently specific physico-chemical properties (that has high tendency to influence its drying characteristics) and therefore different from other investigated tomatoes varieties in the literature. Also, commercial pre-treatment methods such as steam and water blanching have not been documented for processing Cobra 26 F1 tomatoes, and suitability or otherwise of GPR models has not been reported for the prediction of Cobra 26 F1 tomatoes drying process, to the best of our knowledge. Therefore, the objectives of this study were to (i) determine the influence of thermal pre-treatment at different drying temperatures on the drying profile of Cobra 26 F1 tomatoes in a convective dryer, (ii) determine the associated drying properties, such as effective diffusivity, activation energy, total energy and specific energy requirements of the thermally pre-treated and raw Cobra 26 F1 tomatoes, and (iii) assess the suitability of GPR to model and predict the experimental kinetic data of both pre-treated and raw Cobra 26 F1 tomatoes as function of drying temperature and time.

MATERIALS AND METHODS

1. Raw Materials

Freshly harvested mature Cobra 26 F1 tomatoes were obtained from a local farm in Omu-Aran, Kwara State Nigeria. The variety of the tomatoes was later confirmed at the Botany unit of the Department of Biological Science of Landmark University Omu-Aran Nigeria. When received in the laboratory, the tomatoes were carefully sorted and only the healthy and firm ones with the same radius (approximately 45 mm) were selected for drying experiments. They were later cleaned and washed with water to remove adhering dirt. Then the tomatoes were wiped with cloths to remove adhering water and cut into cylindrical slab geometry with thickness of 6 mm. Both the diameters and thicknesses of the slices were measured using a vernier calliper.

2. Steam and Hot Water Blanching Pre-treatments of Cobra 26 F1 Tomato Slabs

Steam and hot water blanching of cylindrical slabs of Cobra 26 F1 tomatoes were carried out by exposing the slab surfaces to steam in a blancher and dipping tomatoes slabs into hot water of 80 °C, respectively, for 5 min. Both the steamed blanched (SB) and hot water blanched (WB) tomatoes were carefully removed from the steam blancher and water baths, respectively, after the allotted residence time and were blotted with tissue paper to remove the excess water at the surfaces. The blanched tomatoes were then allowed to cool to room temperature before further processing.

3. Drying Process and Drying Data Analysis

The effect of drying temperature on the drying behavior of unblanched, hot water and steam blanched tomatoes was conducted in a hot air laboratory convective oven (Stangas SG-90526, Stangas Italy) available in the Department of Chemical Engineering, Landmark University Nigeria. Oven drying temperatures selected

for the drying operations were 40, 50, 60 and 70 °C, while constant drying air velocity of 1.2 m/s was used. This selected temperature range fell within the reported air drying temperatures of food and agricultural produce [1-4]. Before the commencement of the drying process, the dryer was run at the experimental drying temperature for at least 30 min to achieve steady state conditions. Then, a Cobra 26 F1 unblanched (UB), SB and WB sample of approximately 7 g (±0.5 g) was placed on the drying tray. The sample moisture loss was recorded at 10 min intervals at the beginning of the experiment and 30 min interval at the last stage of the experiment by discontinuously weighing the experimental sample on digital scales (with a ±0.01 g precision) till a constant weight was obtained. In the course of experimentation, however, errors that could result from human, instruments, environment and procedures were envisaged and therefore each drying experiment was performed twice. The means of the drying data were, however, used to construct the drying curves [3,6,7,11,13]. The initial moisture content of the Cobra 26 F1 UB, SB and WB samples was determined by using the oven drying method at 105 °C for 5 h (AOAC, 1990). The mean of initial moisture content was found to be 94.49%, 94.65%, 94.80% wet basis (wb g/g) for UB, SB and WB slabs. During the drying data analysis, the moisture content (wb g/g) and moisture ratio of the UB, SB and WB cylindrical slabs were calculated by using Eq. (1) and (2), respectively.

$$M = \frac{W_w - D_w}{W_w} * 100 \tag{1}$$

$$MR = \frac{M - M_{eq}}{M_o - M_{eq}} \tag{2}$$

where, W_w, D_w, MR, M, M_0, M_{eq} are the wet weight (g), dry weight (g), moisture ratio, moisture content at any time (wb g/g), initial moisture content (wb g/g) and equilibrium moisture content (wb g/g), respectively, of UB, SB and WB slabs.

4. Determination of Effective Moisture Diffusivity

Drying data of the UB, SB and WB Cobra 26 F1 tomato slabs were interpreted using Fick's second law of mass diffusion and Eq. (3) was the analytical solution of Fick's equation according to Doymaz [10].

$$MR = \frac{8}{\pi^2}\Sigma_{n=1}^{\infty}\frac{1}{(2n-1)^2}\exp\left(-\frac{(2n-1)^2\pi^2 D_{eff}t}{4l}\right) \tag{3}$$

Since the drying time was long enough to reach equilibrium moisture content, Eq. (3) was simplified and Eq. (4) resulted.

$$MR = \frac{8}{\pi^2}\exp\left(-\frac{\pi^2 D_{eff}t}{4l^2}\right) \tag{4}$$

Eq. (4) was linearized to obtain Eq. (5) and the effective moisture diffusivity was estimated from the slope (k_o) (Eq. (6)) of the plot of In(MR) versus drying time (t).

$$In(MR) = \ln\left(\frac{8}{\pi^2}\right) - \left(\frac{D_{eff}\pi^2}{4L^2}D_t\right) \tag{5}$$

$$k_o = \frac{\pi^2 D_{eff}}{4L^2} \tag{6}$$

D_{eff} is the effective moisture diffusivity (m^2/s), l is the half thickness of tomato slab (m), and D_t is drying time (s).

5. Determination of Activation Energy

Aregbesola et al. [26] presented the temperature dependence of effective diffusivity by Arrhenius relationship as:

$$D_{eff} = D_o\exp\left(-\frac{E_a}{RT}\right) \tag{7}$$

where D_o is the pre-exponential factor of the Arrhenius equation (m^2/s); E_a the activation energy (kJ/mol); R the universal gas constant (kJ/mol K) and T is the absolute air temperature (K).

Eq. (7) was linearized by taking the natural logarithm of Arrhenius equation and this resulted in Eq. (8).

$$\ln(D_{eff}) = \ln D_o - \frac{E_a}{R(T)} \tag{8}$$

The minimum amount of energy required to initiate moisture diffusion (Activation energy) of sample tomatoes slabs was determined from the slope of the straight line of $In(D_{eff})$ versus 1/T.

6. Determination of Total and Specific Energy Consumption for Tomato Slabs Drying

The total energy and the specific energy requirements for drying UB, SB and WB Cobra 26 F1 tomato slabs at different air temperatures in a batch convective oven were calculated using the experimental data as expressed in Eq. (9)-(10) [27].

$$E_t = Av\rho_a c_a \Delta T D_t \tag{9}$$

$$E_s = \frac{E_t}{W_0} \tag{10}$$

where E_t, E_s, A, v, ρ_a, c_a, ΔT, D_t, and W_o are the total needed energy for drying at each condition of the experiments, specific energy consumption, the tray area, air velocity, the air density, specific heat capacity of the drying air, temperature difference, drying time and initial weight, respectively.

Both the total and specific energy requirements for all investigated UB, SB and WB Cobra 26 F1 tomato slabs at different air temperatures were reported as mean and standard deviation.

7. Modelling the drying of UB, SB and WB Cobra 26 F1 Slabs

7-1. GPR-based Modeling Theory

Gaussian process (GP) is a stochastic process that involves the collection of random variables, such that all random variables have joint multivariate normal distribution. GP modelling is a probabilistic type that fits all observable data points by a line. A regression that uses GP to fit interpolated data is known as Gaussian process regression (GPR). Lin et al. [23] presented Eq. (11) as a representation of a function that follows a GP.

$$f(x) \sim GP(\mu(x), k(x, x')) \tag{11}$$

Two important parameters that define a GP are its mean function ($\mu(x)$) and covariance (which is also referred to as kernel function) (k(x, x'). Note that x and x′ refer to spatial location of inputs. The GP $\mu(x)$ and k(x, x') are presented in Eq. (12) and Eq. (13).

$$\mu(x) = \mathbb{E}[f(x)] \tag{12}$$

$$k(x, x') = \mathbb{E}[(f(x) - \mu(\mathbf{x}))(f(\mathbf{x}') - \mu(\mathbf{x}'))] \tag{13}$$

where $\mathbb{E}$ represents the expected value of the argument in the

brackets.

The above expressions indicate that the characteristic of GP is wholly defined by k(x, x′). The selection of k(x, x′) is very important during the training process of a GP model since it is the parameter that helps in defining a smooth and flexible f(x) [24]. The different types of k(x, x′) defined in the literature are squared-exponential kernel (Eq. (14)), rational quadratic kernel (Eq. (15)), periodic kernel (Eq. (16)) and Matérn kernel (Eq. (17)) [25].

$$k_{SE}(x, x') = \sigma_o^2 \exp(-(x-x')^2/2\lambda^2) \tag{14}$$

$$k_{RQ}(x, x') = \sigma_o^2 (1+(x-x')^2/2a\lambda^2)^{-\alpha} \tag{15}$$

$$k_{P_{er}}(x, x') = \sigma_o^2 \exp\left(\frac{2\sin^2(\pi(x, x')/P)}{\lambda^2}\right) \tag{16}$$

$$k_{M_z}(x, x') = \sigma_o^2 \frac{1}{2^{z-1}\Gamma(z)} \left(\sqrt{2z}\frac{|x, x'|}{\lambda}\right)^z \cdot B_z\left(\sqrt{2z}\frac{|x, x'|}{\lambda}\right) \tag{17}$$

where σ_o is the amplitude and λ is the correlation length characteristic. P in Eq. (16) is the period in the function to be learned. Parameters Γ and B_z in Eq. (17) are the standard Gamma function and modified Bessel function of second kind of order z. Parameter z controls the degree of regularity of resultant GP.

By taking z=1/2, 3/2 and 5/2, respectively, in Eq. (17), the exponential kernel (Eq. (18)), Matérn 3/2 kernel (Eq. (19)) and Matérn 5/2 kernel (Eq. (20)) are also obtained.

$$K_E(x, x') = \sigma_o^2 \exp(-|x-x'|/\lambda|) \tag{18}$$

$$k_{M_{3/2}}(x, x') = \sigma_o^2 \left(1+\sqrt{3}\frac{|x-x'|}{\lambda}\right) \cdot \exp\left(-\sqrt{3}\frac{|x-x'|}{\lambda}\right) \tag{19}$$

$$k_{M_{5/2}}(x, x') = \sigma_o^2 \left(1+\sqrt{5}\frac{|x-x'|}{\lambda}+\sqrt{5}\frac{(x-x')^2}{3\lambda^2}\right) \cdot \exp\left(-\sqrt{5}\frac{|x-x'|}{\lambda}\right) \tag{20}$$

GPR is a flexible non-parametric modeling that finds distribution over the possible function f(x) that is consistent with the observed data [25]. When modeling in GPR, the Bayesian approach in function space view is used for the estimation of the distribution of f(x) [28]. The linear regression model according to Bayesian inference in both function space and weight space is presented in Eq. (21).

$$y = f(x) + \varepsilon \tag{21}$$

where x is the input, f is the regression function, y is the observed value and $\varepsilon \sim N(0, \sigma_\varepsilon^2)$ is an independent distributed Gaussian noise.

The principle of GPR is to compute f(x) in Eq. (21) using the set of input and output variables. The f values (also known as prior) are assumed to have normal distribution and conform to Eq. (11). GP modeling starts with a prior distribution and it updates the prior as new data points are observed, thereby producing a posterior distribution over the function. GPR accomplishes this by approximating Eq. (11) using a set of observed training data, n, D={(x_i, y_i), 1≤i≤n)}. The input (x_i) and output (y_i) vectors and are put together into matrix $X \in R^{n \times D}$ and $y \in R^{n \times 1}$, respectively, so that the training data set can be obtained as (X, y).

Therefore, it can be written from Eq. (21) that:

$$y \sim N(\mu(x), K + \sigma_\varepsilon^2 I) \tag{22}$$

Here, $K=k(X, X) \in R^{n \times n}$ and I is identity matrix. The joint distribution of **y** (observed data) and latent noise-free function on the test point $f_*=f(X_*)$ is represented in Eq. (23).

$$\begin{bmatrix} y \\ f_* \end{bmatrix} \sim N\left(\begin{bmatrix} \mu(X) \\ \mu(X_*) \end{bmatrix}, \begin{bmatrix} K+\sigma_\varepsilon^2 I & K_* \\ K_*^T & K_{**} \end{bmatrix}\right) \tag{23}$$

where $K_*=k(X, X_*) \in R^{n \times n}$ and $k_{**}=k(X_*, X_*) \in R^{n_* \times n_*}$

The posterior predictive density is also Gaussian [29] and it is represented in Eq. (24):

$$\mathbf{f}_* | \mathbf{X}, \mathbf{y}, \mathbf{X}_* \sim N(\mu_*, \sigma_*^2) \tag{24}$$

where,

$$\mu_* = \mu(\mathbf{X}_*) + \mathbf{K}_*^T(\mathbf{K}+\boldsymbol{\sigma}^2\mathbf{I})^{-1}(\mathbf{y}-\mu(\mathbf{X})) \tag{25}$$

$$\boldsymbol{\sigma}_*^2 = \mathbf{K}_{**} - \mathbf{K}_*^T(\mathbf{K}+\boldsymbol{\sigma}_\varepsilon^2\mathbf{I})^{-1}\mathbf{K}_* \tag{26}$$

The μ_* and $\boldsymbol{\sigma}_*^2$ in Eq. (25) and Eq. (26) are the posterior mean and covariance, respectively. Covariance function (kernel) has parameters called hyperparameters which can be estimated during model training by maximization of the marginal log-likelihood or the cross validation method. The marginal log-likelihood equation is presented in Eq. (27).

$$\log - \text{likelihood} = \Sigma_{i=1}^n \log\left(\frac{1}{\sigma\sqrt{2}} e^{-\frac{1}{2}\left(\frac{y_i-\mu}{\sigma}\right)^2}\right) \tag{27}$$

where log denotes the natural logarithm, σ is the standard deviation, y is the function value of observed data and μ is the mean of model.

7-2. GPR-based Model Development

The experimental drying data of UB, SB and WB tomato slabs were divided into training (seen) and testing (unseen) data. GPR models were thereafter developed and trained with the seen experimental drying kinetics data of UB, SB and WB tomatoes using Gaussian processes for machine learning library (GPML) available in MATLAB 2017 environment. The trained GPR models were thereafter used for the prediction of seen, unseen and all (seen and unseen) experimental drying data of UB, SB and WB Cobra 26 F1 tomato slabs. The input data were the drying temperature and time, while the response was the moisture ratio. The four kernels that were examined for defining GPs used for the purpose of modeling Cobra 26 F1 experimental moisture ratio are the squared-exponential kernel, rational quadratic kernel, Matérn kernel and exponential kernel. The cross validation method that is available in the MATLAB 2017 was adopted for the optimization of the examined kernel hyperparameters and prevention of over fitting. The statistical parameters employed for judging model accuracy were the root mean square error (RSME), coefficient of determination values (R^2) and mean absolute error (MAE) and are as defined in Eq. (28)-(30).

$$RMSE = \sqrt{\frac{1}{n}\Sigma_{i=1}^n (y_i - y^*)^2} \tag{28}$$

$$R^2 = 1 - \frac{\Sigma_{i=1}^n (y_i - y^*)^2}{\Sigma_{i=1}^n (y_i - y)^2} \tag{29}$$

$$MAE = \frac{1}{n}\Sigma_{i=1}^{n}\left|y_i - y^*\right| \quad (30)$$

where, y_i, y^*, y and n are observed, predicted output, mean of the observed and number of observations, respectively.

RESULTS AND DISCUSSION

1. Effect of Air Drying Temperature on Characteristics of UB, SB and WB Slabs

The profiles of Cobra 26 F1 tomato slabs at constant air drying velocity of 1.2 m/s and different temperatures for UB, SB and WB samples are shown in Fig. 1. It is apparent that moisture ratio decreased with increased drying time. The moisture ratio was observed to have higher dependence on drying time at the beginning of drying compared with the latter stage of drying. Furthermore, air drying temperature was observed to have a notable effect on drying. As can be observed from Fig. 1, tomato slabs dried at higher temperatures tended to reach equilibrium faster than counterparts processed at lower temperatures. This could be attributed to increased moisture evaporation rate at higher air drying temperatures as a result of reduced relative humidity induced around the samples compared to drying at lower temperatures. Also, the drying profile does not exhibit constant rate drying period and the drying took place entirely at the falling drying period. This implies that the mechanism of moisture movement in tomato slabs was predominantly diffusion. The same was observed in agricultural produce like plantain [27].

The influence of sample pre-treatment is well observed in Fig. 1. Fig. 1(b) and (c) represent drying curves of tomato slabs blanched with steam and hot water for 5 min, respectively. It is interesting that both steam and water blanching caused significant reduction in drying time as compared to UB samples (Fig. 1(a)).

As can be seen from the drying curves, the total time required for achieving moisture ratio of 0.01 in UB samples was approximately 500 min at 40 °C, while it took approximately 420 min to achieve a similar result at the same drying conditions for both SB and WB samples. Both steam and hot water blanching pre-treatments have the potential of shortening the drying time of tomatoes slabs up to 16%, and this could have significant effect on the energy economics of the process. Similar trend of positive drying time shortening was observed for other drying temperatures for

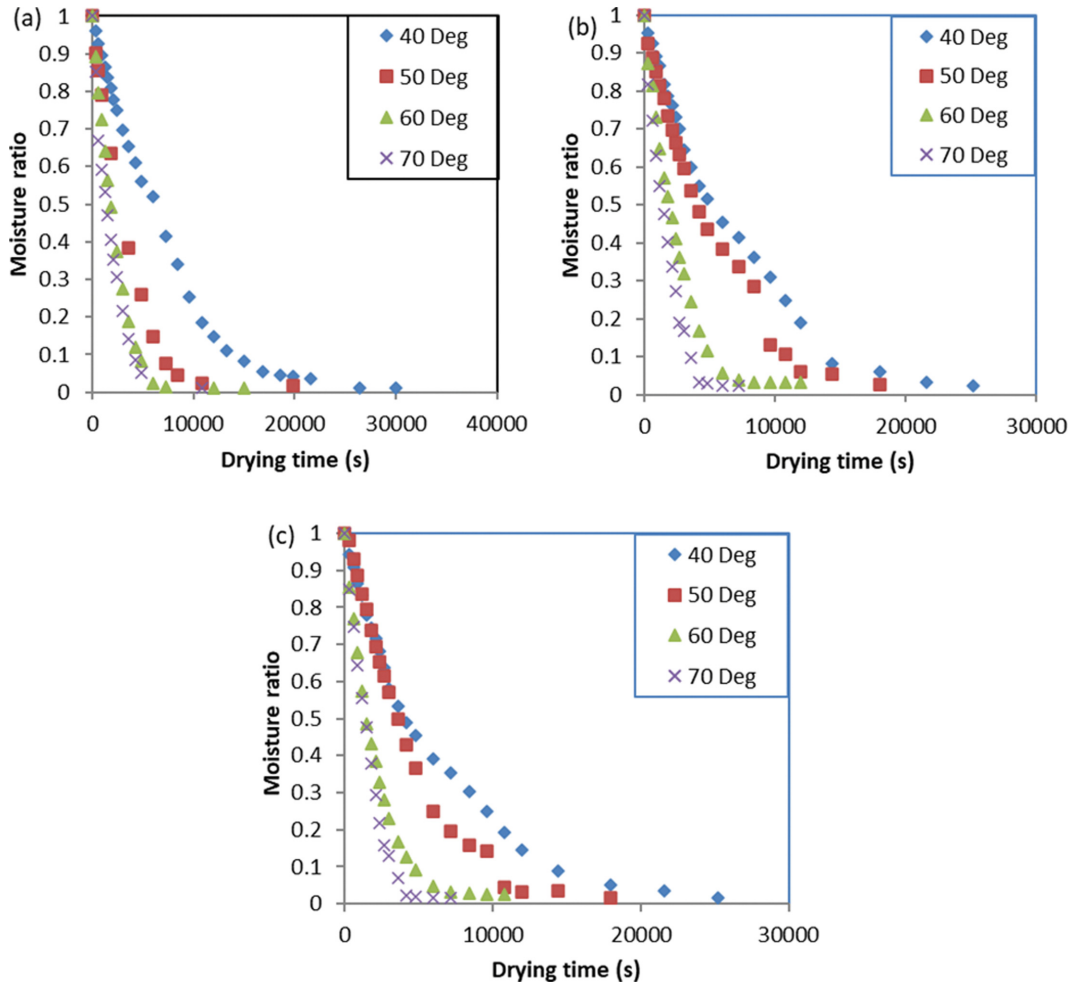

Fig. 1. Drying profile of Cobra 26 F1 (a) UB (b) SB (c) WB (UB - unblanched tomatoes; SB - steam blanched tomatoes; WB - hot water blanched).

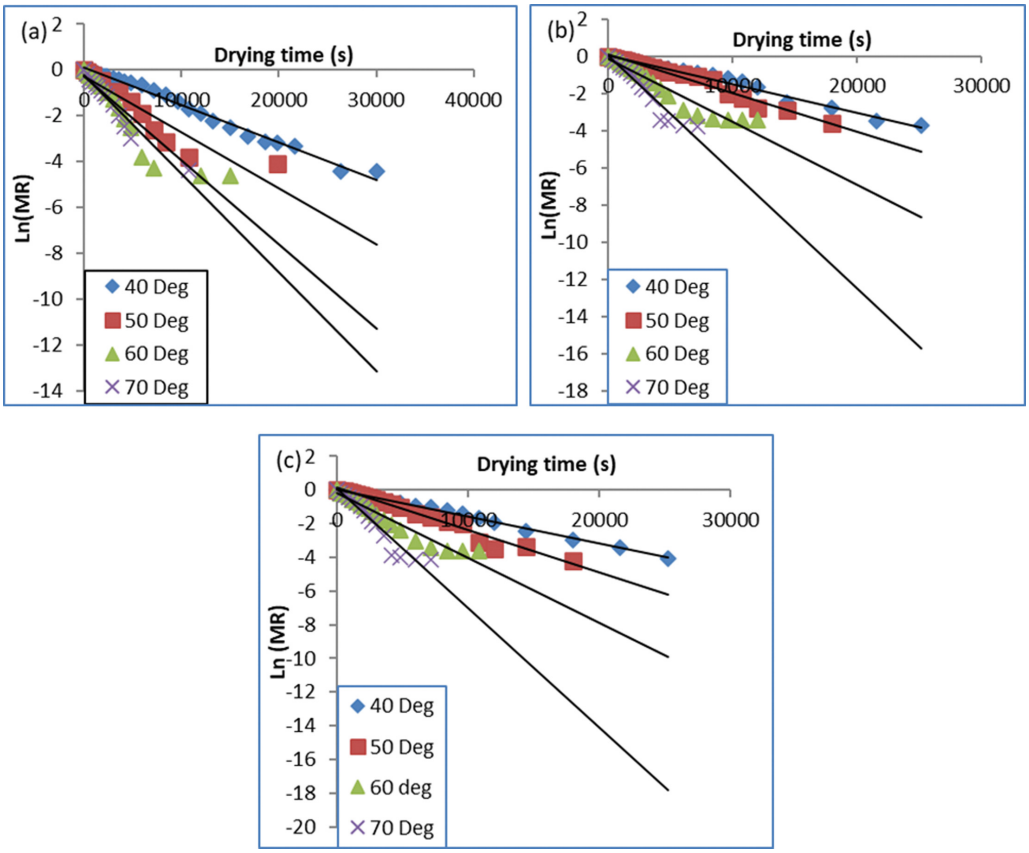

Fig. 2. In (MR) vs. t for Cobra 26 F1 tomatoes (a) UB (b) SB (c) WB (UB - unblanched tomatoes; SB - steam blanched tomatoes; WB - hot water blanched).

Table 1. Values of effective diffusivity obtained for Cobra 26 F1 UB, SB and WB at different drying temperatures

UB			
Temperature (°C)	Effective diffusivity (D_{eff}) (m^2/s)	Equation of fit	R^2
40	3.6466 E -10	−0.0001x+0.0970	0.9896
50	7.2932 E -10	−0.0002x+0.2550	0.8727
60	1.0939 E -09	−0.0003x+0.2854	0.8640
70	1.4586 E -09	−0.0004x+0.2035	0.9456
SB			
Temperature (°C)	Effective diffusivity (D_{eff}) (m^2/s)	Equation of fit	R^2
40	7.2932 E -10	−0.0002x+0.0689	0.9865
50	7.2932 E -10	−0.0002x+0.0854	0.9770
60	1.0939 E -09	−0.0003x+0.1565	0.9327
70	1.8233 E -09	−0.0005x+0.0403	0.9392
WB			
Temperature (°C)	Effective diffusivity (D_{eff}) (m^2/s)	Equation of fit	R^2
40	7.2932 E -10	−0.0002x+0.0035	0.9964
50	1.0939 E -09	−0.0003x+0.1338	0.9754
60	1.4586 E -09	−0.0004x+0.2039	0.9500
70	2.5526 E -09	−0.0007x+0.0825	0.9310

the blanched tomatoes compared with unbleached samples. Decreased drying time observed with blanched tomatoes samples at all drying temperatures could be attributed to loosening of the cellular network, which consequently resulted in more softening tissue during drying [5]. It is, however, noteworthy that both the steam and hot water blanching pre-treatments have comparable drying profiles and beneficial effects. Similar observation of decrease in drying time with pre-treatments of seedless grapes [30], cherry tomato [31] and Goji berries [32] was reported.

2. Effective Moisture Diffusivity of UB, SB and WB Slabs

The effective moisture diffusivity (D_{eff}) of UB, SB and WB samples was determined at different air drying temperatures from the slope of a plot of In (MR) versus drying time (t) in Fig. 2. The D_{eff} values of unblanched and blanched tomatoes and their respective equation of fit are as shown in Table 1. The R^2 values for all the equations of fit were high, which indicated good fit between the experimental and predicted data and were between 0.8640 and 0.9964, making them appropriate for the estimation of D_{eff}. Similar approach was used to estimate D_{eff} of some agricultural produce like seedless grapes [30], bell pepper [3], and garlic slices [33].

The D_{eff} values of the UB, SB and WB Cobra 26 F1 tomatoes in Table 1 ranged between 3.6466 E -10 and 1.4586 E -09 m^2/s; 7.2932 E -10 and 1.8233 E -09 m^2/s; 7.2932 E -10 and 2.5526 E -09 m^2/s, respectively. The values of D_{eff} obtained lie between 10^{-12} to 10^{-8} m^2/s for drying of food materials [31]. Tomato slabs blanched with hot water and dried at 70 °C and UB dried at 40 °C had the highest and lowest D_{eff}, respectively. It is clear from Table 1 that D_{eff} increased with an increase in drying temperature for all categories of treatments. This is in agreement with the report of Tunde-Akintunde et al. [3] on the effect of pre-treatments on the drying characteristics of bell pepper and in confirmation that increase in drying temperature does increase the moisture diffusion and shortens drying time.

Blanching pre-treatments also affected the mean D_{eff} values of the dried tomatoes compared with the unbalanced tomatoes. From the table, the mean D_{eff} values of steam and hot water blanched tomatoes were higher than their corresponding unblanched counterparts dried at the same conditions.

3. Activation Energy and Energy Requirements of Cobra 26 F1 UB, SB and WB

The activation energy, which is the energy needed to initiate diffusion of moisture from the core of the material, was estimated from slope of the plot of $\ln D_{eff}$ versus 1/T as presented in Eq. 8. The plots of $\ln D_{eff}$ versus 1/T for UB, SB and WB samples are presented in Fig. 3. The graphs that were obtained from the plots were all straight lines and this indicated Arrhenius relationships.

The activation energy ranged from 27.86 to 43.65 kJ/mol with the highest (43.65 kJ/mol) belonging to UB, while SB samples had the least of 27.86 kJ/mol. The activation energy for WB samples was 36.01 kJ/mol. The results of this study compare well with activation energy of untreated and pre-treated bell pepper, which varied from 39.59 to 83.87 kJ/mol [3]. The activation energy values obtained were within the general range of 12.7-110 kJ/mol for food materials [12]. Both the steam and water pre-treatments had significant reduction effects on the activation energy when compared with the UB. The relatively low activation energy implied that less

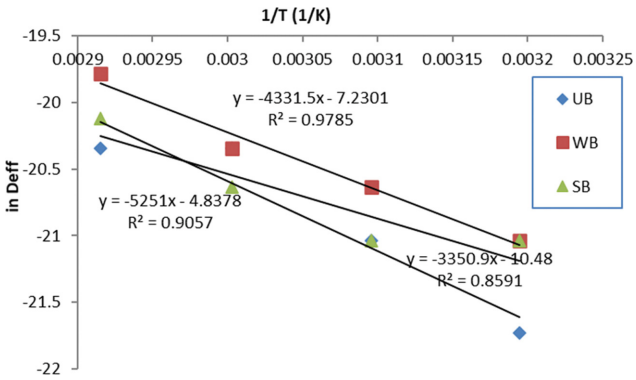

Fig. 3. Influence of air temperature on the effective diffusivity of UB, SB and WB (UB - unblanched tomatoes; SB - steam blanched tomatoes; WB - hot water blanched).

energy is needed to initiate moisture transfer in the tomato samples. Tunde-Akintunde [27] reported similar observation of activation energy lowering effect due to sample pre-treatment; however, a contrary increase was reported by Cheng et al. [5] on the effect of blanching on cherry tomatoes.

To further analyze the effect of pre-treatment on the energy economics of the process, the total energy that is required for the drying of one charge and specific energy (energy required for drying 1 kg) of UB, SB and WB slabs at all experimental conditions were calculated using Eqs. (9) and (10), respectively. Fig. 4 and Fig. 5 present the plots of the total and specific energy requirements for all drying temperatures, respectively. Fig. 4 and Fig. 5 show that both total and specific energy requirements decreased with increased drying temperature for UB, SB and WB samples. Cobra 26 F1 tomato sample pre-treatment and drying conditions have affected both total and specific energy differently. The mean total and specific energy at all drying conditions and for UB, SB and WB samples was in the range of 7.08-18.33 kWh and 1,069.12-2,768.80 kWh/kg, respectively. The SB and WB had the lowest values for both total and specific energy at 70 °C, while UB had the highest

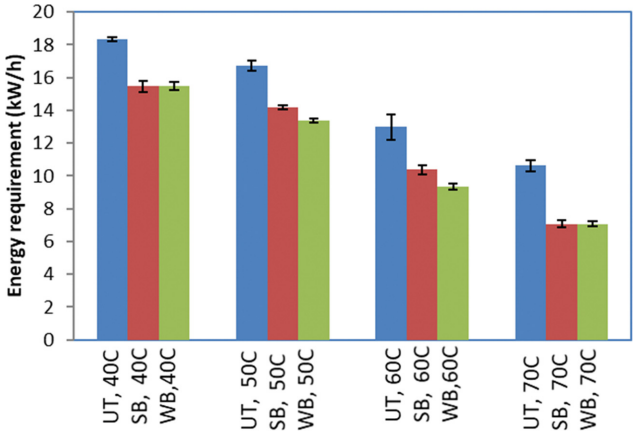

Fig. 4. Total energy requirement for drying of Cobra 26 F1 slabs (UB - unblanched tomatoes; SB - steam blanched tomatoes; WB - hot water blanched).

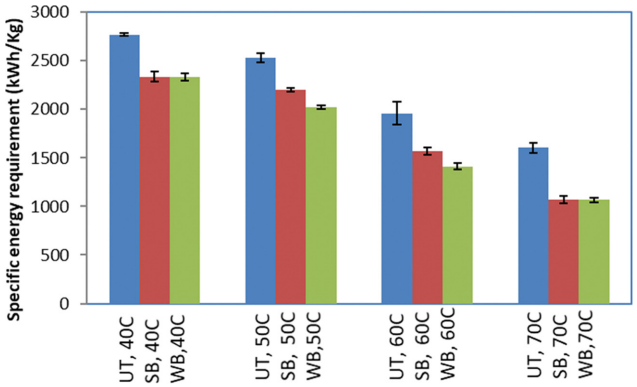

Fig. 5. Specific energy requirement for drying of Cobra 26F1 slabs (UB - unblanched tomatoes; SB - steam blanched tomatoes; WB - hot water blanched tomatoes.

total and specific energy values at 40 °C drying temperature. Also, the values of total and specific energy values for blanched tomatoes are lower than the UB at all drying conditions. This implies that increased drying temperatures and blanching greatly reduced the energy utilization during drying as a result of increased moisture diffusion and evaporation from the internal region and material surface, respectively, thus assisting in drying process optimization [27].

It was observed that SB samples possessed lower amount of activation energy when compared with WB samples. However, the total and specific energy requirements for WB samples were higher than the SB samples at 50 and 60 °C and were the same at 40 and 70 °C. The wide disparity in SB, WB and UB activation energies implied that pre-treatment had notable effects on the relaxation (loosening or softening) of tomato tissue structure. In the process of steam blanching of tomato samples, the steam had probably affected the surface tomatoes tissues more severely than the tissues in the core, and hence SB had uneven tissue relaxation from the sample surface to the core. However, during the hot water blanching, hot water had longer range penetrating effects of relaxing the tomato structure since samples were totally submerged in the hot water, and hence WB samples had more evenly relaxed tissue structure throughout the samples. In the process of drying the two samples (SB and WB), therefore, it was probably easier to remove moisture easily with less energy from a severely affected SB surfaces than a more evenly relaxed tissue structure surfaces of WB. Therefore, it is expected that the activation energy of SB will be lower than that of WB.

Regarding the specific and total energy of SB and WB, it can be observed from Fig. 1 that the cumulative effect of both steam and water blanching shortened the drying time for up to 16%, and both SB and WB had similar and comparable drying profiles. This shortened drying time of SB and WB samples had a remarkable effect on their energy requirements. The evenly relaxed (loosened) tissue structures of WB encouraged moisture diffusion from the whole tomato samples (both at the surface and the core), and hence cumulatively shortened the drying time more than the SB samples with unevenly relaxed tissue structures (severely relaxed at the tomatoes slab surface and not very relaxed at the core) because of short penetrating effect of the stream treatment. Hence, both the total and specific energy requirements of the WB are appreciably lower at 50 and 60 °C drying temperatures than that of SB. However, the total and specific energy requirements were similar at 40 and 70 °C probably because the low drying temperature of 40 °C reasonably increased the drying time of SB and WB samples needed to overcome the moisture resistances in the tissues of the tomatoes. Similarly, the high drying temperature of 70 °C, increased the drying rate and was able to overcome the moisture resistance that could result from tomato structural hindrances for both SB and WB slabs. Although, both specific and energy requirements of SB and WB samples at these temperatures were marked with moderately high standard deviations as observed in Fig. 4 and Fig. 5. The D_{eff} of SB and WB at these temperatures (40 and 70 °C) were also comparable as shown in Table 1.

4. Descriptive Statistics and GPR Modelling of Drying Data of UB, SB and WB Samples

The descriptive statistics of the drying data were investigated prior to the GPR modelling to understand comprehensively the data characteristics and variability. The drying data used as input for

Table 2. Descriptive statistics of the input and output experimental variables

Statistical parameters	Drying temperature (°C)	Drying time (s)	Moisture ratio
Mean	53.17391	5,010	0.444465
Standard Error	0.741805	353.5232	0.021503
Median	50	3,000	0.420639
Mode	40	0	1
Standard Deviation	11.25004	5,361.445	0.326107
Sample Variance	126.5635	28,745,096	0.106346
Kurtosis	−1.34911	2.923909	−1.35009
Skewness	0.203193	1.727249	0.164958
Range	30	26,400	0.989941
Minimum	40	0	0.010059
Maximum	70	26,400	1
Sum	12,230	1,152,300	102.2269
Count	230	230	230

Table 3. Parameters for training different GPR-based model types (Seen data)

GPR-based type	RMSE	R^2	MAE	Prediction speed (obs/s)	Training time (s)
GPR-RQ	0.05	0.980	0.03	330	31.434
GPR-SE	0.06	0.970	0.03	330	28.046
GPR-M 5/2	**0.04**	**0.999**	**0.02**	**1,700**	**32.133**
GPR-Ex	0.05	0.970	0.03	1,700	31.516

GPR-RQ=GPR defined with rational quadratic kernel; GPR-SE=GPR defined with squared-exponential kernel; GPR-Ex=GPR defined with squared-exponential kernel; GPR-M5/2=GPR defined with Matérn 5/2 kernel.

the GPR modelling were the drying temperature and drying time, while the response/output variable was moisture ratio. Note that both blanched and unblanched drying data were taken into consideration during drying data analysis and GPR modelling. Some of the statistical parameters considered during analysis were the mean, standard error, median, mode, standard deviation, sample variance, kurtosis, skewness, range, minimum and maximum. Table 2 presents the results of the descriptive statistical analysis of the convective drying data of SB, WB and UB Cobra 26 F1 tomato slabs.

The total data population used for model training and prediction is 690, which represents 230 data count each for drying temperature, drying time and moisture ratio. The mean, median and mode for drying temperature, drying time and moisture ratio were 53.17391, 50, 40; 5,010, 3,000, 0 and 0.444465, 0.420639, 1, respectively. Also, the minimum and maximum datum for drying temperature, drying time and moisture ratio were 40 and 70, 0 and 26,400, and 0.010059 and 1, respectively. The standard error and standard deviation ranged from 0.021503-353.5232 and 0.326107-28,745,096, respectively, for all the data set. The sample variance of 28,745,096 and 126.5635 for drying time and drying temperature implied wide variations, while 0.106346 for moisture ratio implied moderate data variation. The skewness and kurtosis statistical parameters indicate the degree of distortion from normal distribution of a data set and whether the data set is light or heavy tailed relative to a normal distribution, respectively [34]. The kurtosis of −1.34911-2.923909 and skewness of 0.164958-1.727249 indicated that the data sets of drying time, drying temperature and moisture ratio are normally distributed, although 2.923909 for drying time in Table 2 implies that the distribution is peaked since the kurtosis value is greater than +1.

The GPR-based models defined with squared-exponential kernel (GPR-SE), rational quadratic kernel (GPR-RQ), Matérn 5/2 kernel (GPR-M 5/2) and exponential kernel (GPR-Ex) were adopted for the training and prediction of convective experimental drying data of SB, WB and UB Cobra 26 F1 tomato slabs. The GPR-based models that were trained learned the relationship between the input variable (drying time and drying temperature) and response variable (moisture ratio) of UB, SB and WB tomato slabs. Table 3 presents the performance of all the GPR-based models used for the training, learning and prediction of moisture ratio of UB, SB and WB tomato slabs as function of drying temperature and time.

The R^2, RMSE and MAE ranged between 0.970-0.999; 0.04-0.06; and 0.02-0.03, respectively. The prediction speed is between 330-1,700 and training time is between 28.046-32.133. Table 3 shows that all GPR-based models were able to learn and predict the training data (comprising 115 data each of drying temperature, time and moisture ratio) with high accuracy (high R^2 value, low RMSE and MAE). The prediction speed and training time are also high and low, respectively, for all the investigated GPR-based models. This indicates that all of the tested kernels are suitable for the learning and prediction of experimental drying data of UB, SB and WB tomato slabs. However, a GPR-based model defined with Matérn 5/2 kernel (GPR-M5/2) was marginally better, having the highest R^2 value (0.999) and lowest RMSE (RMSE=0.04) and MAE (MAE=0.02) values. The training time of 32.133 sec is also relatively low and has high prediction rate of 1,700 obs/s when compared with others.

The optimum beta and sigma hyperparameter values for the

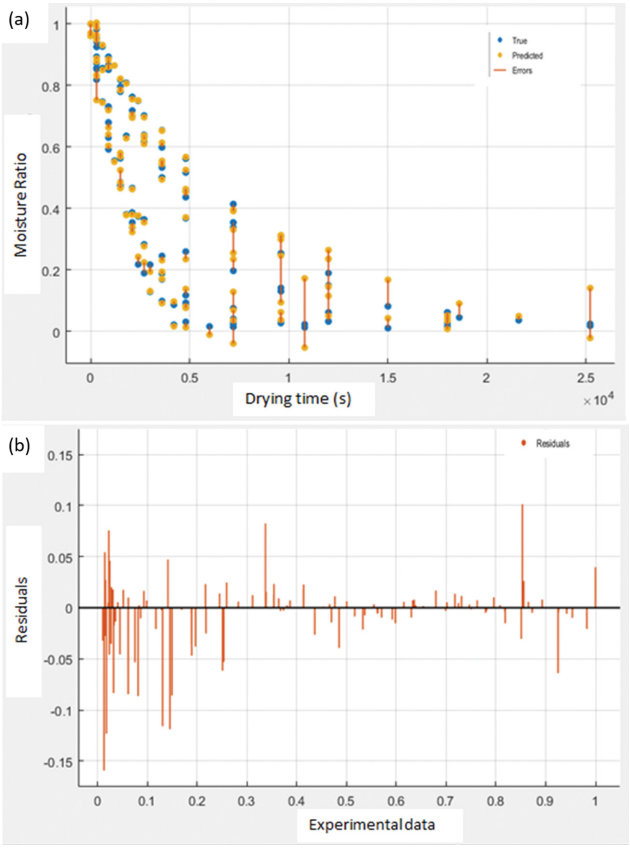

Fig. 6. (a) Response plot for training and predicted data (b) residuals against experimental moisture ratio data plot using GPR-M5/2.

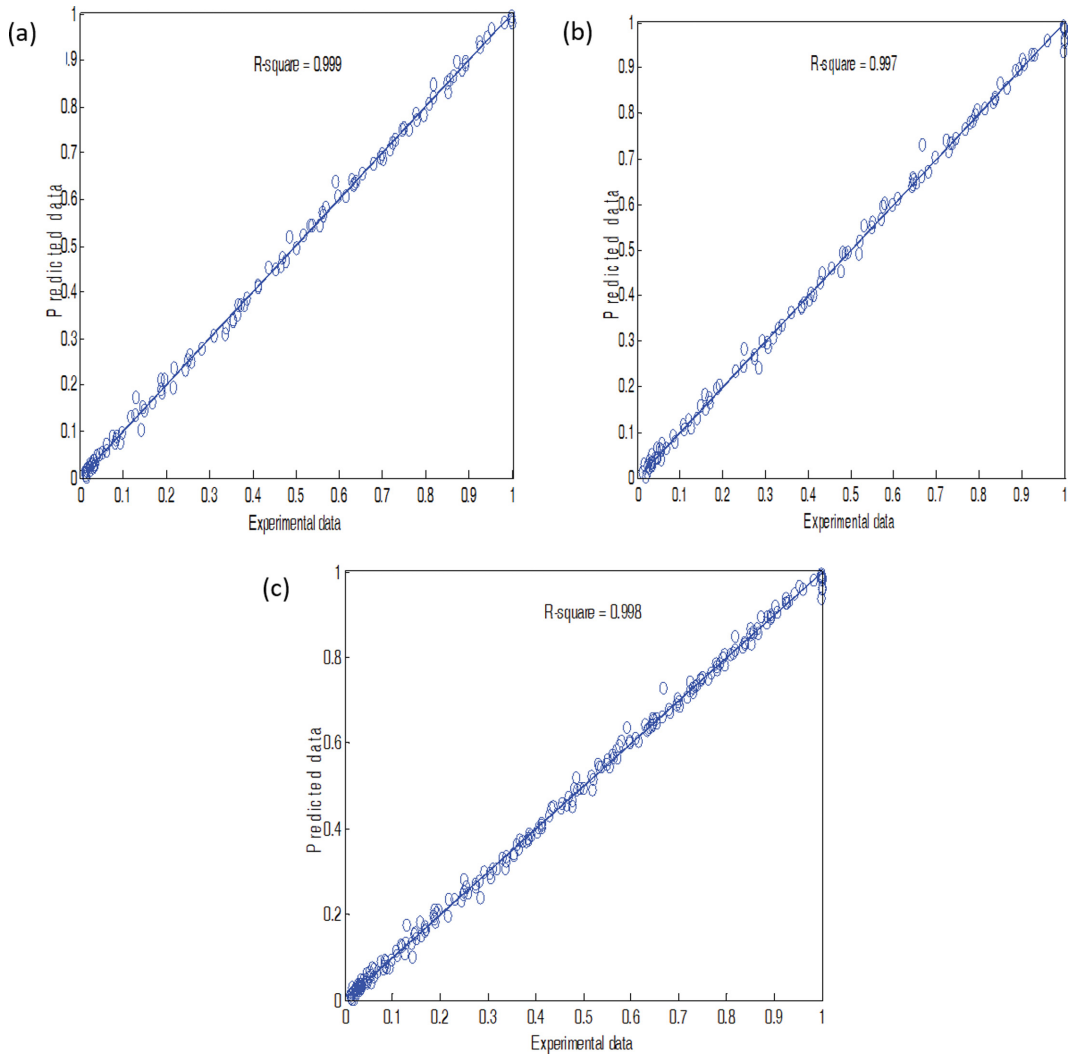

Fig. 7. Comparison between experimental and predicted moisture ratio using GPR-M5/2 model for (a) seen data, (b) unseen data, (c) all data.

trained GPR-M5/2 are 1.81023 and 0.01334, respectively, while the kernel amplitude (σ_o) and correlation length characteristic (λ) are 3.62024 and 1.79208, respectively. Fig. 6(a) shows the response plot for the training and predicted data, while Fig. 6(b) is the residuals plot of the experimental moisture ratio for GPR-M5/2 prediction.

As indicated in Fig. 6(a), the blue dots represent the experimental training data, the red dots are the GPR-M5/2 predicted training data, while the red solid line represents the difference between the experimental training data and predicted training data (error). The error was quantified for each data point prediction as shown in the figure. As seen in Fig. 6(a) is the disparity between the experimental and predicted varied and can be viewed in Fig. 6(b). Fig. 6(b) is the residual (error) plot for all the experimental moisture ratio data. The thick black line in Fig. 6(b) represents the zero line, while the residuals above and below the line represent larger and smaller values data prediction of the GPR-M5/2 than the experimental moisture ratio data. The closer the residual to the base zero line, the better the prediction of GPR-M5/2. As can be observed in Fig. 6(b), the errors between the experimental and GPR-M5/2 predicted data are small (the highest residual above the line being 0.1, while the least below the line is less than 0.16), which represents an excellent fit.

The robustness of the trained GPR-M5/2 was tested by using the model to predict the seen, unseen and all data (both seen and unseen data). Fig. 7 is the parity graphs for the experimental and predicted data for the seen, unseen and all data points.

Both the experimental and predicted moisture ratio data were distributed around the center line in Fig. 7 for seen, unseen and all data, signifying perfect fitness. The R^2 value for the trained GPR-M5/2 prediction of seen, unseen and all experimental data was 0.999, 0.997 and 0.998, respectively. The RMSE for the seen, unseen and all data was 0.042, 0.047 and 0.043, respectively. The MAE for seen data was 0.021, for unseen data was 0.025 and for all data predictions was 0.022. It is therefore clear from Fig. 7 that GPR-M 5/2 shows good representation of the experimental moisture ratio and is able to predict with high accuracy. Chaurasia et al. [19] also reported GPR-based models to predict drying time of mosambi peel with very high accuracy.

CONCLUSION

The influence of steam blanching, hot water blanching and drying temperature on the thin layer drying characteristics of Cobra 26 F1 tomato slabs was investigated in a convective dryer. Drying data obtained for the pre-treated and un-blanched samples were thereafter modelled and predicted by using Gaussian process regression-based models. Blanching and drying temperature of Cobra 26 F1 tomatoes had notable influence on the drying time, moisture diffusivity, activation energy, total energy and specific energy requirements. All the drying curves did not show constant rate drying period, and drying predominantly took place in the falling rate period; therefore, drying of blanched and unblanched Cobra 26 F1 tomatoes could be said to be driven mainly by diffusion. All the Gaussian process regression-based models employed for the modelling and prediction of experimental kinetic data of blanched and unblanched Cobra 26 F1 tomatoes were suitable. However, the Gaussian process regression-based model defined with Matérn 5/2 kernel was marginally better. Therefore, it can be concluded that steam and water blanching and high drying temperature can improve the processing and energy economics of drying of Cobra 26 F1 tomatoes. Gaussian process regression-based models can be used during the robust controller design for monitoring and control of Cobra 26 F1 tomatoes drying in a convective dryer.

FUNDING

This work did not receive any funds either from public, commercial or not-for-profit grant agencies.

DECLARATION OF COMPETING INTEREST

Authors have no conflicts of interest to declare.

REFERENCES

1. R. A. Iyanda, A. O. Adeboye and K. A. Yusuf, *An. Univ. "Eftimie Murgu"*, **21**, 1 (2014).
2. P. A. Idah, J. J. Musa, and S. T. Olaleye, *AU J.T.*, **14**, 1 (2010).
3. T. T. Akintunde, B. O. Akintunde and A. Fagbeja, *Afr. J. Food Agric. Nutr. Dev.*, **11**, 7 (2011).
4. E. K. Akpinar and S. Toraman, *Heat Mass Transf.*, **52**, 10 (2015).
5. L. S. Cheng, S. Fang and M. L. Ruan, *Int. J. Food Eng.*, **11**, 2 (2015).
6. A. R. P. Kingsly, R. Singh, R. K. Goyal and D. B. Singh, *Am. J. Food Technol.*, **2**, 2 (2007).
7. O. Adeyi, A. J. Adeyi and O. E. Oke, *NSChE J.*, **33**, 1 (2018).
8. F. Karimi, S. Rafiee, A. Taheri-Garavand and M. Karimi, *J. Taiwan Inst. Chem. E*, **43**, 1 (2012).
9. S. B. Mariem, S. B. Mabrouk and M. Khan, *Int. J. Energy Eng.*, **4**, 17 (2014).
10. I. Doymaz,. *J. Food Eng.*, **78**, 4 (2007).
11. J. O. Ojediran, C. E. Okonkwo, A. J. Adeyi, O. Adeyi, A. F. Olaniran, N. E. George and A. T. Olayanju, *Heliyon*, **6**, 3 (2020).
12. J. B. Stamatios and G. B. Vassilios, *J. Food Eng.*, **65**, 449 (2004).
13. T. Tunde-Akintunde, O. Oyelade and B. Akintunde, *Agric. Eng. Int.: CIGR J.*, **16**, 2 (2014).
14. M. Kaveh, V. R. Sharabiani, R. A. Chayjan, E. Taghinezhad, Y. Abbaspour-Gilandeh and I. Golpour, *Inf. Process. Agric.*, **5**, 3 (2018).
15. N. R. Sahoo, M. L. Bal, S. U. Pal and D. Sahoo, *Food Technol. Biotechnol.*, **53**, 1 (2015).
16. S. E. Agarry, *TURJAF*, **4**, 10 (2016).
17. X. Sun, X. Jin, N. Fu and X. Chen, *Food Sci. Nutr.*, **8**, 11 (2020).
18. U. Garba, S. Kaur, S. Gurumayum and P. Rasane, *Food Technol. Biotechnol.*, **53**, 3 (2015).
19. P. Chaurasia, K. Younis, O. S. Qadri, G. Srivastava and K. Osama, *J. Food Process Eng.*, **42**, 2 (2019).
20. Y. Tao, Y. Li, R. Zhou, D. T. Chu, L. Su, Y. Han and J. Zhou, *J. Food Sci. Technol.*, **53**, 10 (2016).
21. S. M. Jafari, M. Ganje, D. Dehnad and V. Ghanbari, *J. Food Process. Preserv.*, **40**, 2 (2016).
22. L. Zhou, J. Chen and Z. Song, *Math Probl Eng.*, **2015**, 1 (2015).
23. C. Lin, T. Li, S. Chen, X. Liu, C. Lin and S. Liang, *Neural Comput. Appl.*, **31**, 12 (2019).
24. S. Shabani, S. Samadianfard, M. T. Sattari, A. Mosavi, S. Shamshirband, T. Kmet and A. R. Várkonyi-Kóczy, *Atmosphere*, **11**, 1 (2020).
25. H. Tolba, N. Dkhili, J. Nou, J. Eynard, S. Thil and S. Grieu, *IFAC-PapersOnLine*, **52**, 4 (2019).
26. O. A. Aregbesola, B. S. Ogunsina, A. E. Sofolahan and N. N. Chime, *Niger. Food J.*, **33**, 1 (2015).
27. T. Y. Tunde-Akintunde, *J. Food Process. Preserv.*, **38**, 4 (2014).
28. A. M. Kotlar, B. V. Iversen and Q. de Jong van Lier, *Vadose Zone J.*, **18**, 1 (2019).
29. M. Lázaro-Gredilla, J. Quiñonero-Candela, C. E. Rasmussen and A. R. Figueiras-Vidal, *J. Mach. Learn. Res.*, **11**, 1865 (2010).
30. İ. Doymaz and P. Altıner, *Food Sci. Biotechnol.*, **21**, 1 (2012).
31. A. S. Kipcak, *Int. J. Therm. Eng.*, **4**, 1 (2018).
32. J. Ni, C. Ding, Y. Zhang and Z. Song, *Innov. Food Sci. Emerg. Technol.*, **61**, 102318 (2020).
33. E. E. Abano, H. Ma, W. Qu and E. Teye, *Afr. J. Food Sci.*, **5**, 7 (2011).
34. A. D. Ho and C. C. Yu, *Educ Psychol Meas.*, **75**, 3 (2015).